

# Design, Development and Analysis of a Voltage Sensor Based on Capacitive Voltage Divider for Smart Grid Applications

Joao Soares Farias Neto, Lucas Vinicius Hartmann,\*  
Camila Seibel Gehrke and Fabiano Salvadori\*

\* *Federal University of Paraiba, Brazil, (e-mail: joão.soares,  
lucas.hartmann, camila, salvadori.fabiano@cear.ufpb.br).*

---

**Abstract:** With the recent push for renewable energy several former consumers units now have energy generation capabilities. While this approach is beneficial in general, it also poses new challenges for cooperation and grid stability. The new smartgrid now needs bidirectional power flow, data communication, and intelligent controls in order to ensure reliable operation. Voltage sensing plays a key role, capacitive voltage transformers have been demonstrated useful for high-voltage (100 kV+), but have not yet been discussed for low (220 V) and medium (13 kV) voltage. This paper proposes a simplified capacitive voltage divider circuit for low-voltage measurement. Mathematical modelling is used for characterization of steady-state operation, circuit design, and sensitivity to component tolerances. Monte-Carlo simulations are employed to verify the effect of component tolerances, indicating under 0.7 dB gain, and 0.03° error at fundamental frequency. Experimental validation is performed at low-voltage levels (127 V), indicating 0.5 dB magnitude and 0.3° phase deviation at fundamental frequency. Performance is also validated from 60 Hz to the 50<sup>th</sup> harmonic, showing 20° phase deviation at the higher order harmonics (16<sup>th</sup> and up). From the obtained results it is expected that the sensor is sufficient for voltage quality measurements, but should be software-corrected if power measurement is required at the high-order harmonics.

*Keywords:* Capacitive Voltage Divider, Smart Grid, Voltage Sensor.

---

## 1. INTRODUCTION

In the past few years a paradigm shift in the electrical grid has being witnessed. With the increasing popularization of renewable energy sources former consumers can now also generate energy. The system that was previously only capable of energy transmission in a single direction, from power plants to consumers, now has to adapt to dynamic power flow and to the increased variability of power from sources such as solar and wind. In order to ensure proper grid operation while still enabling the use of cleaner, distributed, energy sources, investments in monitoring and intelligent control are decisive. This new paradigm of electrical grid, where ubiquitous monitoring and control are exploited as tools to improve energy management, is denominated Smart Grid, see Salvadori et al. (2017).

In general, the understanding of smart grid can be summarized in three main pillars: Information Technology, Distributed Intelligence and Communication, and Control and Automation Systems, see Borlase (2012). The progress of researches and the development of these technologies has challenged the stability of the electricity grid system, since, these advances cause an increase in energy flows together with the non-linear loads connected to the grid. The improvement of the network does not occur automatically and instantly with the inclusion of this intelligence, given that, this not only makes networks intelligent, but also increases the vulnerability of the network to instabilities

caused by inadequate routines. This problem demands the construction of an improved measurement instrumentation system to monitoring and control the status of the smart grid, see Rietveld et al. (2014).

Capacitive voltage transformers (CVT) have been reliably used in high voltage measurement applications for over 70 years, see Freiburg et al. (2016). These devices are composed of a capacitive voltage divider followed by an inductive transformer stage, are commonly used for measurement of transmission line voltages in excess of 100 kV, and have been subject of several characterizations studies, see Brehm et al. (2017); Chen et al. (2013); Sule et al. (2006); Cong et al. (2018). In a smart grid scenario with end-users injecting power along the distribution networks, a more widespread voltage monitoring would be desired. One interesting CVT alternative for low-voltage (100-240 V) distribution networks is shown in Ren et al. (2018), where a non-contact probing is done through parasitic capacitive coupling to the voltage rails, and no inductive transformer stage is employed. While still sufficient for the proposed wattmeter, the variability of the parasitic capacitive coupling adds considerable uncertainties to the voltage measurement.

In this paper a differential voltage sensor based on capacitive voltage divider for distribution networks is investigated. Mathematical modelling is demonstrated for analysis, including sensitivity to manufacturing tolerances,

and the design procedure is presented. Simulation and experimental results are shown to characterize and validate the sensor.

## 2. CIRCUIT MODELLING AND DESIGN

### 2.1 Capacitive Voltage Divider Circuit

The principle of voltage sensor is show in Fig. 1. The capacitive potential divider circuit was designed so that the voltage levels of a three-phase load can be adjusted to safe operating levels for the acquisition system that operate with voltages from 0 V to 3 V.  $V_{off}$  is a DC source for offset injection. During the initial part of the modeling it was considered  $V_{off} = 0$ .

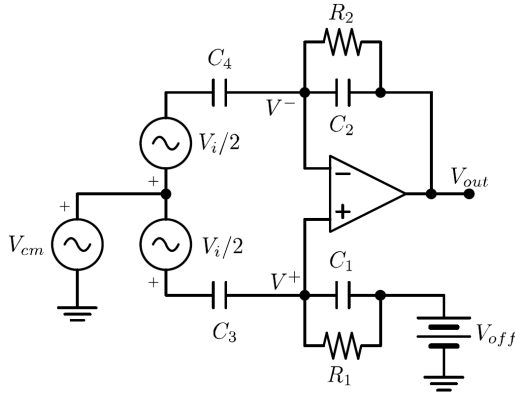


Figure 1. Capacitive voltage divider circuit.

From the circuit of Fig. 1, using the voltage method of electrical circuit analysis nodes, it is possible to determine the output voltage  $V_{out}$  based on the input voltages  $V_i$  and the inverter configuration of the operational amplifier, allowing the dimensioning of the components used in the project. From the assumption of the virtual short circuit, we got for the positive and negative terminal of the operational amplifier the transfer function equations (2) and (4) respectively.

$$V^+ = \frac{(V_{cm} + V_i/2)Z_1 + V_{off}Z_3}{Z_1 + Z_3} \quad (1)$$

$$V^+ = \frac{(2C_3R_1V_{cm} + C_3R_1V_i)s}{(2C_1R_1 + 2C_3R_1)s + 2} \quad (2)$$

$$V^- = \frac{(V_{cm} - V_i/2)Z_2 + V_{out}Z_4}{Z_2 + Z_4} \quad (3)$$

$$V^- = \frac{(2C_4R_2V_{cm} - C_4R_2V_i + 2C_2R_2V_{out})s + 2V_{out}}{(2C_2R_2 + 2C_4R_2)s + 2} \quad (4)$$

In normal operation of the amplifier the voltages at the positive and negative terminals are the same. With that, we developed equations (2) and (4) and determined the transfer functions of output voltage relations by the input voltage and common mode voltage.

$V_i$  is the voltage desired to be measured and  $V_{cm}$  is considered an undesired disturbance in the circuit. In order to eliminate this common mode voltage, the following

conditions was defined:  $R_2 = R_1$ ,  $C_2 = C_1$  and  $C_4 = C_3$ . Therefore, the common mode component was eliminated and we got a simplified transfer function of  $V_{out}/V_i$  in the equations (5).

$$\frac{V_{out}}{V_i} = \frac{(C_3R_1)s}{(C_1R_1)s + 1} \quad (5)$$

As the circuit is linear, the  $V_{out} / V_{off}$  transfer function can be combined with  $V_{out} / V_i$  by superposition. Thus, it can be observed in equation (6) this relationship under real conditions.

$$A = C_1C_2R_1R_2 + C_1C_4R_1R_2.$$

$$B = C_1C_2R_1R_2 + C_2C_3R_1R_2.$$

$$\frac{V_{out}}{V_{off}} = \frac{As^2 + (C_1R_1 + C_2R_2 + C_4R_2)s + 1}{Bs^2 + (C_1R_2 + C_2R_2 + C_3R_1)s + 1} \quad (6)$$

As  $V_{off}$  is a DC voltage source, when  $s = 0$ , the expression (6) behaves as in ideal conditions, reducing to expression (7).

$$\frac{V_{out}}{V_{off}} = 1 \quad (7)$$

### 2.2 Designing of Passive Components

The transfer function of a first-order high pass filter, as well as the frequency response of the filter and the module of  $(j\omega)$  is given by equations (8) and (9) respectively, and the cutoff frequency by equation (10).

$$F(s) = \frac{sRC}{sRC + 1} \rightarrow F(j\omega) = \frac{j\omega RC}{j\omega RC + 1} \quad (8)$$

$$|F(j\omega)| = \frac{|j\omega RC|}{|j\omega RC + 1|} = \frac{\omega RC}{\sqrt{\omega^2 R^2 C^2 + 1}} \quad (9)$$

$$|F(j\omega)| = \frac{\omega_c RC}{\sqrt{\omega_c^2 R^2 C^2 + 1}} = \frac{1}{\sqrt{2}} \rightarrow \omega_c = \frac{1}{RC} \quad (10)$$

The cutoff frequency must be less than 60 Hz for our applications. The gain is given by the ratio of the output voltage to the input voltage. The conditioning circuit was designed to have a gain that reduces the mains voltage from 622  $V_{pp}$  to a maximum of 3  $V_{pp}$ . Thus, considering  $C_1R_1\omega \gg 1$ , the gain in the pass band is given by equation (11).

$$\frac{V_{out}}{V_i} = \frac{C_3R_1s}{C_1R_1s + 1} = \frac{3}{622} = \frac{C_3R_1s}{C_1R_1s} \quad (11)$$

Admitting  $s = j\omega$  and  $\omega = 2\pi f$ , with the grid frequency at 60 Hz, the  $R_1$  value is determined by the equation (13).

$$C_3R_12\pi f = 622 \quad (12)$$

$$R_1 = \frac{622}{C_32\pi f} \quad (13)$$

Assuming the value of  $C_3 = 270 \text{ nF}$ , and replacing in equation (13), we got the numeric value of  $R_1$  expressed in (14).

$$R_1 = \frac{622}{270 \cdot 10^{-9} \cdot 2\pi 60} = 6.1139 \cdot 10^6 \cong 6 \text{ M}\Omega \quad (14)$$

The conditioning circuit simulation was performed using an input voltage similar to the grid voltage, this being  $311 V_{peak}$ , and we observing the voltage levels at the circuit output. The simulation result is exposed on Fig. 2.

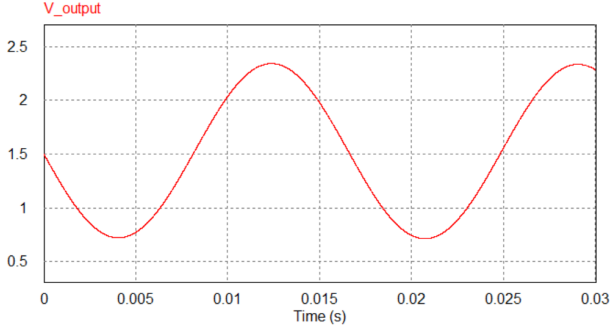


Figure 2. Simulation of the proposed voltage circuit using the PSIM software.

### 3. SENSITIVITY ANALYSIS

#### 3.1 Sensitivity Mathematical Theory

The sensitivity analysis procedure is relevant, since it is possible to classify in levels of efficiency, the influence of the parameters on the functional output of the model, Opalski (2015). Sensitivity is a measure of the variation degree in the performance of a system, due to variations that occur in the parameters that affect the transfer function of the system, Daryanani and Daryanani (1976). Consider a filter transfer function expressed in terms of the parameters  $\omega_p$ ,  $\omega_z$ ,  $Q_p$ ,  $Q_z$  and  $K$ , in the form:

$$T(s) = K \cdot \frac{s^2 + \frac{\omega_z}{Q_z}s + \omega_z^2}{s^2 + \frac{\omega_p}{Q_p}s + \omega_p^2} \quad (15)$$

where,  $\omega_p$  and  $\omega_z$  are the cut frequency pole,  $Q_p$  and  $Q_z$  are the quality factor and  $K$  is the voltage gain. For a better understanding, admit a network where we want to identify the sensitivity of the frequency pole  $\omega_p$ , due a variation in a resistor  $R$  that compose the grid. The pole sensitivity is defined as the change per unit in the frequency pole caused by a change per unit in the resistor  $R$ . Mathematically:

$$S_R^{\omega_p} = \lim_{\Delta R \rightarrow 0} \frac{\frac{\Delta \omega_p}{\omega_p}}{\frac{\Delta R}{R}} = \frac{R}{\omega_p} \frac{\partial \omega_p}{\partial R} \quad (16)$$

$$S_R^{\omega_p} = \frac{\partial(\ln \omega_p)}{\partial(\ln R)} \quad (17)$$

However, the system proposed in this work is composed by a capacitive and resistive network. Thus, it is interesting to realize the sensitivity analysis given the simultaneous variation of all the elements that compose the circuit. This

analysis is done expanding the desired parameter calculus in a Taylor series, Daryanani and Daryanani (1976):

$$\Delta \omega_p = \frac{\partial \omega_p}{\partial x_1} \Delta x_1 + \frac{\partial \omega_p}{\partial x_2} \Delta x_2 + \dots + \frac{\partial \omega_p}{\partial x_m} \Delta x_m \quad (18)$$

+ second order terms and higher order terms.

Where  $m$  is the total number of elements in the circuit. Since the variations in the elements are considered small, the second order and higher order terms can be ignored Daryanani and Daryanani (1976). Thus, we have:

$$\Delta \omega_p \cong \sum_{j=1}^m \left( \frac{\partial \omega_p}{\partial x_j} \right) \Delta x_j \quad (19)$$

$$\Delta \omega_p \cong \sum_{j=1}^m \left( \frac{\partial \omega_p}{\partial x_j} \frac{x_j}{\omega_p} \right) \left( \frac{\Delta x_j}{x_j} \right) \omega_p \quad (20)$$

$$\Delta \omega_p \cong \sum_{j=1}^m S_{x_j}^{\omega_p} V_{x_j} \omega_p \quad (21)$$

Where,  $V_{x_j}$  is the change per unit of element  $x_j$ . Therefore, it is possible realize the sensitivity analysis of each parameter of the proposed circuit, considering the simultaneous influences of the other elements that compose it.

#### 3.2 Sensitivity Analysis of Circuit Elements

Initially, we must define which parameters we want to perform the sensitivity analysis. In the specific context of the proposed circuit, it will be the gain in the passband for  $V_i$  and  $V_{cm}$ . Since we have a high pass filter we can use  $\omega = \infty$  which is definitely inside the passband. Using the squared gain coefficients of  $\omega$  in these conditions, we will define the necessary equation to determine the sensitivity of each component, that is:

$$\lim_{\omega \rightarrow \infty} \left| \frac{V_{out}}{V_i} \right| = \frac{(C_1 C_4 + C_2 C_3 + 2C_3 C_4)^2}{4C_2^2 (C_1 + C_3)^2} \quad (22)$$

To obtain the equation that defines the circuit sensitivity given the influence of each element, we start from the sensitivity gain equation (22) and then calculate the derivative in relation to the parameter being analyzed and obtain the sensitivity equation for each circuit element. To facilitate, the following definition will be made:

$$\lim_{\omega \rightarrow \infty} \left| \frac{V_{out}}{V_i} \right| = G_{V_o} \quad (23)$$

Thus, we have:

$$S_{C_1}^{G_{V_o}} = \frac{C_1}{G_{V_o}} \frac{\partial G_{V_o}}{\partial C_1} \quad (24)$$

$$S_{C_2}^{G_{V_o}} = \frac{C_2}{G_{V_o}} \frac{\partial G_{V_o}}{\partial C_2} \quad (25)$$

$$S_{C_3}^{G_{V_o}} = \frac{C_3}{G_{V_o}} \frac{\partial G_{V_o}}{\partial C_3} \quad (26)$$

$$S_{C_4}^{G_{V_o}} = \frac{C_4}{G_{V_o}} \frac{\partial G_{V_o}}{\partial C_4} \quad (27)$$

It was developed an algorithm in MATLAB to implement the equations from (24) to (27), providing as the literal results the following equations:

$$S_{C_1}^{G_{V_o}} = \frac{2C_1C_3(C_2 + C_4)}{(C_1 + C_3)(C_1C_4 + C_2C_3 + 2C_3C_4)} \quad (28)$$

$$S_{C_2}^{G_{V_o}} = -\frac{2C_4(C_1 + 2C_3)}{(C_1C_4 + C_2C_3 + 2C_3C_4)} \quad (29)$$

$$S_{C_3}^{G_{V_o}} = \frac{2C_1C_3(C_2 + C_4)}{(C_1 + C_3)(C_1C_4 + C_2C_3 + 2C_3C_4)} \quad (30)$$

$$S_{C_4}^{G_{V_o}} = \frac{2C_4(C_1 + 2C_3)}{(C_1C_4 + C_2C_3 + 2C_3C_4)} \quad (31)$$

Replacing the values of each design component, we obtain the numerical result of each sensitivity:

$$S_{C_1}^{G_{V_o}} = -0.9963 \quad (32)$$

$$S_{C_2}^{G_{V_o}} = -1.0037 \quad (33)$$

$$S_{C_3}^{G_{V_o}} = 0.9963 \quad (34)$$

$$S_{C_4}^{G_{V_o}} = 1.0037 \quad (35)$$

The sensitivity is calculated in PU (per unit), thus, it is observed in the numerical values obtained, that if the capacitors vary by 1%, the output also vary by 1%. For capacitors  $C_1$  and  $C_2$  the vary is inversely proportionally and for  $C_3$  and  $C_4$  the vary is proportionally. In the literature, sensitivities less than or equal to 1% are considered low Daryanani and Daryanani (1976), which implies that the sensitivity of the proposed circuit is satisfactory to our application.

#### 4. MONTE CARLO SIMULATION: COMPONENT TOLERANCE ANALYSIS

The method proposed in this work was used to generate a curve with a uniform probability distribution function in order to analyse the best and worst scenarios of variation in the electronic components value, given their respective tolerances. The algorithm used performed successive simulations considering a tolerance range for each component, providing at the end of the analysis informations about the gain in dB and the phase in degrees, as well as the worst cases of variation in the circuit output. In the statistical analysis performed, the parameters of mean, standard deviation and maximum and minimum values obtained from successive simulations were evaluated.

The result of the gain and phase absolute values of the Monte Carlo simulation are shown in Fig. 3. In the simulation, tolerances of 5% for capacitors and 1% for resistors were considered. However, it is not possible to visualize the gain and phase errors as they are very small. It is observed that at the frequency of 60 Hz the gain is

stable, which means that there may be small variations upwards or downwards that can be improved through calibration.

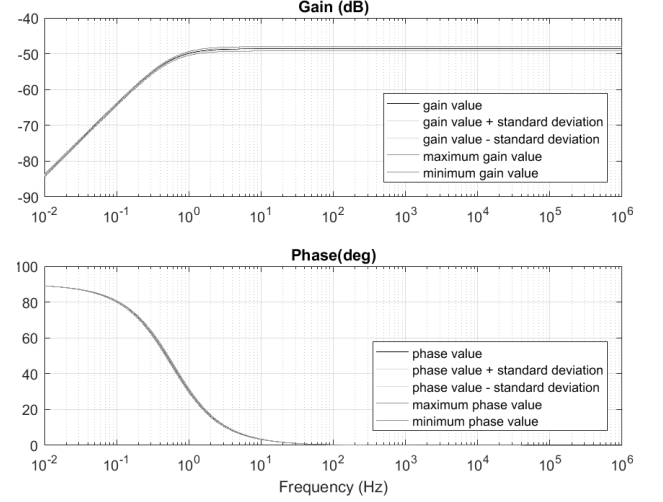


Figure 3. Absolute values obtained in Monte Carlo analysis.

In order to be able to visualize the gain and phase errors of the absolute values, the subtraction of each parameter of the mean was implemented in the algorithm, we can observe the gain and phase errors more clearly. Fig. 4 shows these results.

A phase error of approximately  $-0.025^\circ$  is observed next to 60 Hz, which can be adjusted with software calibration. The line on zero is the subtraction of average value, the two lines closest to zero are the maximum and minimum standard deviation subtracted from average value and the furthest lines from zero are the maximum and minimum gain errors in the first graphic and phase errors values in the second graphic.

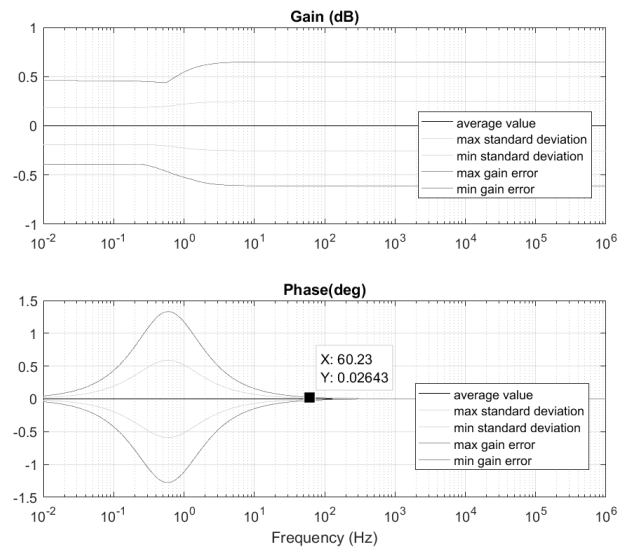


Figure 4. Gain and phase errors in dB and degrees respectively.

## 5. EXPERIMENTAL SETUP AND RESULTS

For the experimental evaluation of the operation of the voltage sensing circuit, the acquisition of the input and output signals were realized in the Laboratory of Research and Optimization of Electrical Systems from Federal University of Paraíba, Brazil, and compared with the results obtained previously in simulation. Initially, the AC signal was acquired directly from the network. The components value used in the circuit were a TL084CN operational amplifier,  $R_1 = R_2 = 6 \text{ M}\Omega$ ,  $C_1 = C_2 = 270 \text{ nF}$ ,  $C_3 = C_4 = 1 \text{ nF}$  and a DC source for offset adjustment of  $V_{off} = 1.5 \text{ V}$ . The workbench used for the tests was composed of two voltage sources for the symmetrical supply of the amplifier and for the offset adjustment, high voltage probes and one oscilloscope.

For protection purposes, a stabilizer with direct input from the network and output at  $110 \text{ V}_{AC}$  was used to evaluate the functioning of the proposed circuit, with the frequency of the network at  $60 \text{ Hz}$ . In Fig. 5, the measured signals can be observed without the offset adjustment, with input voltages at  $326 \text{ V}_{pp}$  and output at  $1.97 \text{ V}_{pp}$ .

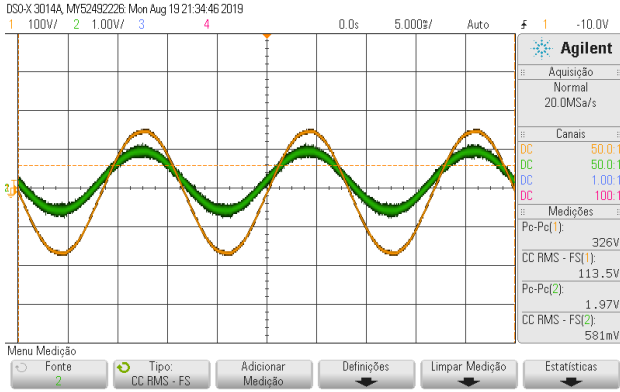


Figure 5. Input and output voltages measurement of the circuit operating.

After the first measurement of the AC signal, the offset adjustment was performed by inserting a DC source with output voltage at  $1.5 \text{ V}_{DC}$ , as done in a simulation, to adjust the amplifier output voltage to positive levels. In Fig. 6, the result of the AC acquisition with the offset adjustment can be seen.

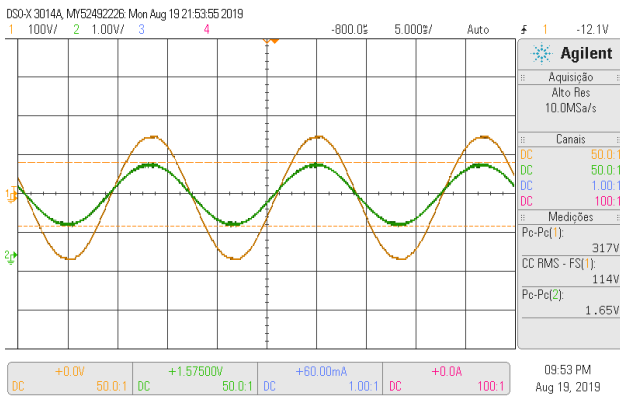


Figure 6. Input and output voltages measurement of circuit with offset adjustment.

The results of the AC measurements were acceptable and compatible with the results obtained in the simulations using the PSIM software, showing good functioning. The gain obtained in the simulation of  $-207.33 \text{ dB}$  approached the real gain of the circuit, which was  $-192.12 \text{ dB}$ .

After this first step of input and output voltage measurements, phase measurements of the output signal were performed using a signal generator varying the frequency from  $1 \text{ Hz}$  to  $500 \text{ kHz}$ . Based on the data obtained from each point that was measured, a graph was constructed using MATLAB to evaluate the difference between the experimental results and the results obtained in simulation. The Fig. 7 shows the phase values obtained experimentally by varying the frequency.

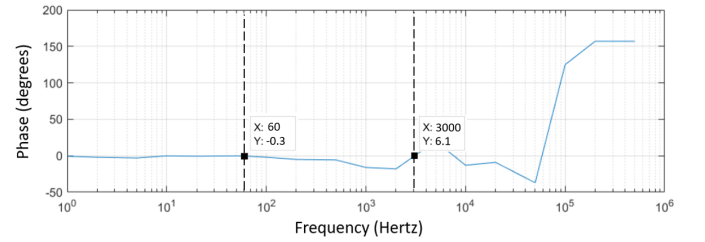


Figure 7. Experimental phase errors for frequency bands from  $1 \text{ Hz}$  to  $500 \text{ kHz}$ .

The phase measurement results varying the frequency differed from the simulation at higher frequencies. For the network frequency,  $60 \text{ Hz}$ , the variation of the measured phase was  $-0.3^\circ$ , which can be explained by the limitations of the measuring equipment.

The limits of region of interest start from the fundamental harmonic at  $60 \text{ Hz}$  to  $3 \text{ kHz}$  of the harmonic of order 50, as required by the Brazilian National Electric Energy Agency (ANEEL). The phase delay remains under  $20^\circ$  over the entire region of interest, and is just  $0.3^\circ$  at the fundamental frequency. This is considered adequate for harmonic distortion monitoring as well as active and reactive power analysis, and can be improved via software compensation if required. The Fig. 8 shows the workbench used in the experiment, as well as the proposed circuit operating.

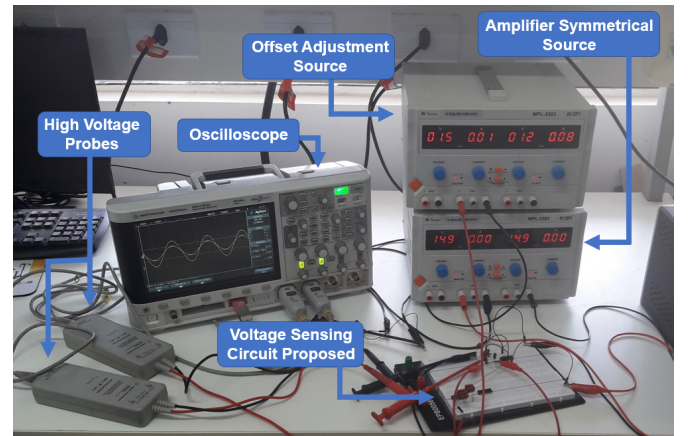


Figure 8. Workbench used for experimental tests.

## 6. CONCLUSION

In this work a differential voltage sensor based on capacitive voltage divider was presented, along with its modelling, analysis, design procedure, and experimental results. Mathematical modelling was employed to demonstrate the circuit's tolerance to component variations, where good sensitivity (close to 1) was obtained for all passive components. The sensitivity analysis was validated via Monte Carlo simulations, where low, stable and limited magnitude and phase errors (under 0.7 dB and  $0.03^\circ$ ) could be observed over the desired frequency range (60 Hz to 3 kHz). Such a flat frequency response allows for simple software calibration routines, while still being sufficient for measurement of 1st to 50th harmonics as required by the Brazilian National Electric Energy Agency (ANEEL) regulations.

Experimental results were provided for 110 V 60 Hz input, and demonstrated output voltage scaling, offset and phase, suitable for connection to a 3.3 V ADC input. Frequency response was also experimentally verified, obtaining  $0.3^\circ$  phase delay at the fundamental frequency (60 Hz). However, at higher order harmonic frequencies (above 1 kHz) the phase error has diverged from simulation, reaching close to  $20^\circ$  in some cases. This behaviour should be further investigated in the future if power analysis is necessary at those frequencies, but is still acceptable for THD and voltage quality measurements.

In the current market there are voltage and current transducers such as LEM for voltage and LV20-P, however, the high price of these sensors often make their use unfeasible. There are commercially available high voltage capacitors in the range of 30 kV, which may enable the same sensor circuit to operate on 13 kV distribution networks. It should be noted that this application requires serious safety considerations, and shall be addressed in a future paper.

## ACKNOWLEDGMENT

The authors would like to thank the Conselho Nacional de Desenvolvimento Científico e Tecnológico (CNPq) for supporting and encouraging scientific initiation and financing of the project process nº 312646/2017-8.

## REFERENCES

- Borlase, S. (2012). *Smart Grid Technologies*, chapter 3. CRC Press. doi:10.1201/b13003-4. URL <https://www.routledgehandbooks.com/doi/10.1201/b13003-4>.
- Brehm, M., Aristoy, G., Trigo, L., Santos, A., and Slomovitz, D. (2017). Errors of capacitive-voltage-transformers used for harmonic measurements. In *2017 IEEE URUCON*, 1–4.
- Chen, S.Q., Li, J.M., Luo, T., Zhou, H.Y., Ma, Q.X., and Du, L. (2013). Study on the impulse characteristics of capacitive voltage transformer. In *2013 IEEE International Conference on Applied Superconductivity and Electromagnetic Devices*, 65–68.
- Cong, Z., Li, P., Xu, H., Liu, C., He, P., and Du, L. (2018). Parameter identification of electromagnetic unit in capacitive voltage transformer. In *2018 International Conference on Diagnostics in Electrical Engineering (Dagnostika)*, 1–4.
- Daryanani, G. and Daryanani, G. (1976). *Principles of Active Network Synthesis and Design*. Wiley. URL <https://books.google.com.br/books?id=sudSAAAAAAAJ>.
- Freiburg, M., Sperling, E., and Predl, F. (2016). Capacitive voltage transformers - electrical performance and effective diagnostic measures. In *2016 International Conference on Condition Monitoring and Diagnosis (CMD)*, 20–23.
- Opalski, L.J. (2015). Efficient global sensitivity analysis method for models of systems with functional outputs. In *2015 European Conference on Circuit Theory and Design (ECCTD)*, 1–4.
- Ren, S., Nakahara, H., Thongpull, K., Phukpattaranont, P., and Chetpattananondh, K. (2018). A development of capacitive voltage sensor for non-intrusive energy meter. In *2018 15th International Conference on Electrical Engineering/Electronics, Computer, Telecommunications and Information Technology (ECTI-CON)*, 776–779.
- Rietveld, G., Braun, J., Wright, P.S., Clarkson, P., and Zisky, N. (2014). Smart grid metrology to support reliable electricity supply. In *29th Conference on Precision Electromagnetic Measurements (CPEM 2014)*, 680–681.
- Salvadori, F., Gehrke, C.S., Hartmann, L.V., de Freitas, I.S., d. S. Santos, T., and Teixeira, T.A. (2017). Design and implementation of a flexible intelligent electronic device for smart grid applications. In *2017 IEEE Industry Applications Society Annual Meeting*, 1–6.
- Sule, I., Aliyu, U.O., and Venayagamoorthy, G.K. (2006). Simulation model for assessing transient performance of capacitive voltage transformers. In *2006 IEEE Power Engineering Society General Meeting*, 4 pp.–.